NJC

Accepted Manuscript

This is an *Accepted Manuscript*, which has been through the Royal Society of Chemistry peer review process and has been accepted for publication.

Accepted Manuscripts are published online shortly after acceptance, before technical editing, formatting and proof reading. Using this free service, authors can make their results available to the community, in citable form, before we publish the edited article. We will replace this *Accepted Manuscript* with the edited and formatted *Advance Article* as soon as it is available.

You can find more information about *Accepted Manuscripts* in the Information for Authors.

Please note that technical editing may introduce minor changes to the text and/or graphics, which may alter content. The journal's standard Terms & Conditions and the Ethical guidelines still apply. In no event shall the Royal Society of Chemistry be held responsible for any errors or omissions in this *Accepted Manuscript* or any consequences arising from the use of any information it contains.

ROYAL SOCIETY OF CHEMISTRY

www.rsc.org/njc

Cite this: DOI: 10.1039/c0xx00000x

www.rsc.org/xxxxxx

ARTICLE TYPE

Enhancing the high-rate performance of $LiFePO_4$ battery with carbonized-filter paper as an interlayer

Zhian Zhang[a*], Zhiyong Zhang[a], Wei Chen[a], Guanchao Wang[a], Jie Li[a], Yanqing Lai[a*]

Received (in XXX, XXX) Xth XXXXXXXXX 20XX, Accepted Xth XXXXXXXXX 20XX

DOI: 10.1039/b000000x

The rate performance of $LiFePO_4$ battery is improved by inserting a carbon interlayer, which is synthesized by a simple, cheap pyrolysis of the filter paper commonly used in the laboratories. The specific capacity of the $LiFePO_4$ battery at low current density is only slightly improved after the introduction of the carbon interlayer, while the specific capacity at high current density is greatly enhanced with a specific capacity of 90 mAh g^{-1} and 76 mAh g^{-1} at 10 C and 20 C, respectively, compared to a specific capacity of 17 mAh g^{-1} and 8 mAh g^{-1} for $LiFePO_4$ battery without a carbon interlayer. The improved electrochemical performance is attributed to the porous architecture of the carbon interlayer, serving as a conductive skeleton, largely reducing the charge transfer resistance.

Introduction

Lithium-ion batteries have rapidly conquered the consumer market of advanced portable electronics in recent years and are now considered as the next generation of power sources for future electric vehicles (EVs), hybrid EVs, and plug-in hybrid EVs [1-4]. Among various lithium-ion batteries being developed for EVs, olivine $LiFePO_4$ seems to be one of the most promising cathode materials because of its advantages of low cost, environmental friendliness, particularly high thermal stability, and strong overcharge tolerance compared with other metal oxides currently used in commercial lithium-ion batteries [5-7]. However, along with these exceptional advantages, olivine $LiFePO_4$ also has the severe disadvantages of very low intrinsic electronic and ionic conductivity, which brings difficulties for high-rate battery applications [8-10].

To improve the rate performance of $LiFePO_4$ based lithium ion battery ($LiFePO_4$ battery), much effort has been made by many academic and industrial laboratories [11-12]. Traditionally, most researches were focused on the active material optimizations to enhance the rate performance, such as coating $LiFePO_4$ particles with carbon materials [13-18], minimizing the $LiFePO_4$ particle size [19-22]. Besides, some attention was also devoted to the advancement of the components of battery electrode, such as binders [23,24]. As discussed, most researches have focused on the modification 'inside' of the cathode, but the design 'outside' of the cathode, such as cell configuration, could be a new strategy for improving the rate performance of $LiFePO_4$ battery. To the best of our knowledge, there is still no report in the literature to enhance the rate performance of $LiFePO_4$ battery by inserting a carbon interlayer between the cathode and the separator.

In this study, we present a cheap and simple, but markedly effectively solution to enhance the rate performance of $LiFePO_4$ battery by inserting a conductive, porous carbon interlayer between the cathode and the separator. As a result, the rate performance of $LiFePO_4$ battery can be greatly improved with a specific capacity of 147 mAh g^{-1}, 90 mAh g^{-1} and 76 mAh g^{-1} at 0.5C, 10 C, 20 C, respectively, which is higher than the specific capacity of the $LiFePO_4$ battery without the carbon interlayer.

Experiment

For preparation of the carbon interlayer, cellulose based filter papers (model 102, Hangzhou Whatman-Xinhua Filter Paper Co., Ltd) with a diameter of 9.0 cm commonly used in laboratory were carbonized in a tube furnace with temperature rising from room temperature to 800 °C at a rate of 5 °C min^{-1} and the temperature was kept at 800 °C for 2 h with the presence of Ar flow of 100 mL min^{-1}. Raman spectra of the dried sample were collected with LABRAM-HR 800 in the range of 2000-1000 cm^{-1} with He-Ne laser excitation at 532 nm. The powder X-ray diffraction (XRD, Rint-2000, Rigaku, Japan) by Cu Kα radiation, was employed to identify the crystalline phase of the prepared samples.

The commercial $LiFePO_4$ powders were provided by Pulead Technology Industry Co., Ltd., China. Super P with an average particle size of 40 nm was acquired from TIMCAL Graphite & Carbon, Switzerland. PVDF (HSV900, M_w=1,000,000) was supplied by Arkema, France. Measured amounts of $LiFePO_4$, Super P and PVDF binder (80:10:10 by mass) were added into a container with suitable amounts of NMP. The components were combined using a Polytron PT 2500E homogenizer at 20000 rpm for 10 min until uniform. The slurry was coated onto aluminium foil current collector (20 μm thickness) by a doctor blade. The laminate loading was controlled by the height of the doctor blade. After the laminate was dried at 50 °C for 30 min to evaporate the solvent, they were cut into wafers with 1.0 cm diameter and were subsequently dried at 110 °C under vacuum for 12 h to remove the residual solvent to obtain $LiFePO_4$ cathode.

Electrochemical performances of the $LiFePO_4$ battery were evaluated in CR2025 coin-type cells, which were assembled using Celgard® 2400 membrane as separator and filled with 70 µL of liquid electrolyte. The lithium electrode in the half cell was used as the counter electrode as well as the reference electrode and the electrolyte is 1 mol L^{-1} $LiPF_6$ dissolved in EC/DMC/EMC 1:1:1 by mass, which was purchased from Zhangjiagang Guotai-Huarong New Chemical Materials Co., Ltd., China. The configuration of the $LiFePO_4$ cell with carbon interlayer was shown in Fig. 1. All the cells were assembled in an argon-filled glove box (Universal 2440/750, Mikrouna Mech. Tech. Co., Ltd.), in which both the water content and the oxygen content are less than 1 ppm.

Charge-discharge performances were measured between 2.5 V and 4.2 V (vs. Li/Li^+) at different current density on Land CT2001A charge/discharge instrument, China. Electrochemical impedance spectra (EIS) of the $LiFePO_4$/Li half cells were tested using PARSTAT 2273 electrochemical measurement system (PerkinElmer Instrument. USA), the frequency window was between 1 MHz and 0.01 Hz, with amplitude of 5 mV. All the tests were conducted at room temperature (25 °C).

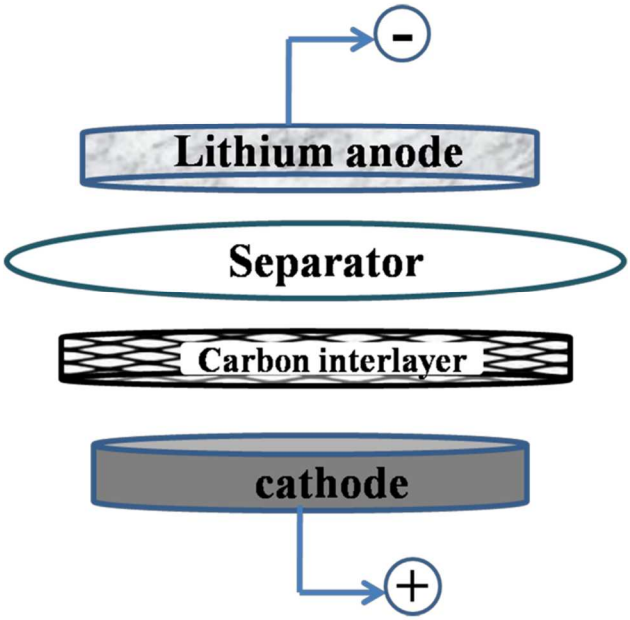

Fig. 1 Configuration of a $LiFePO_4$-based cell with functional carbon interlayer

Results and discussion

Scanning electron micrographs of the surface of the carbon interlayer are presented in Fig. 2. It can be found that the carbon interlayer is primarily composed of carbonized fibers, which is caused by the loss of elements (e.g., O and H) at high temperature. The tortuous carbon fibers construct porous and conductive network structure, which will be filled with liquid electrolytes and may provide a facile pathway for the electron and ion movement. The conductivity of the carbon interlayer measured by four-probe method is 3.47 S m^{-1}. Fig. 2b presents the cross sectional image of the carbon interlayer. It can be found that the thickness of the carbon interlayer is approximately 60 µm.

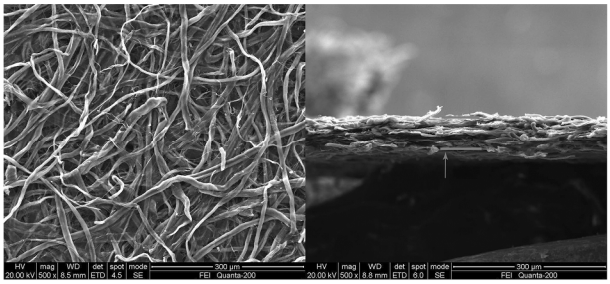

Fig. 2 SEM photographs of the carbon interlayer: (a) surface; (b) cross-section.

The XRD pattern of the carbon interlayer (Fig. 3a) shows the presence of reflections characteristic of carbon hexagonal phase, the broad diffraction peak appears at about 24° and 44° which can be indexed to (002) and (100)/(101) planes, respectively, suggesting the presence of partially graphitized structures of the carbon interlayer [25]. Moreover, the partially graphitized structures of the carbon interlayer could be further supported by Raman spectroscopy (Fig. 3b). Two characteristic peaks around 1340 and 1590 cm^{-1} could be ascribed to D band arising from the defects and disorders in carbonaceous solid and G band from the stretching mode of C-C bonds of typical graphite, respectively [26].

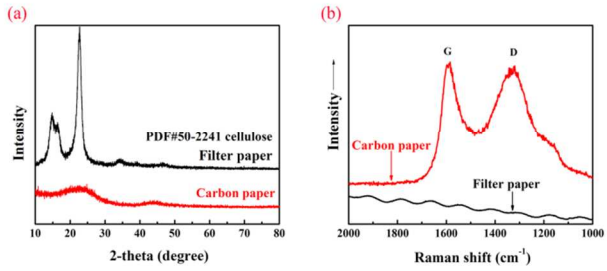

Fig. 3 XRD patterns (a) and Raman spectra (b) of the prepared carbon interlayer

Fig. 4a presents cycle performances of the cell with the carbon interlayer and without the carbon interlayer at the current rate of 1 C (1 C = 175 mA g^{-1}) between 2.5 V and 4.2 V. It can be seen from Fig. 4a that the cell with the carbon interlayer shows higher specific capacity than that of the cell without the carbon interlayer. The discharge capacity of the cell without the carbon interlayer is 120 mAh g^{-1} for the initial cycle and decreases to 118.3 mAh g^{-1} after 100 cycles, which is similar to the others result. [27,28]. Whereas the discharge capacity of the cell with the carbon interlayer is 132.1 mAh g^{-1} for the initial cycle and a high reversible capacity of 131.1 mAh g^{-1} is retained after 100 cycles with the capacity retention ratio of 99.2%.

The rate performance of the cell with or without the carbon interlayer at room temperature is also interesting, as shown in Fig. 4b. The discharge capacity gradually decreases as the current rate rising from 0.5 C to 20 C for both of the cells. It can be found that the cell without the carbon interlayer can only deliver a

specific capacity of 17 mAh g^{-1} and 8 mAh g^{-1} at 10 C and 20 C, respectively, similar to the result reported by previous literatures [29,30]. However, the cell with the carbon interlayer demonstrated a better rate performance with a high specific capacity of 90 mAh g^{-1} and 76 mAh g^{-1} at 10 C and 20 C, respectively. Moreover, the cell with the carbon interlayer can recover most of the capacity when the current rate was reduced back to 1 C. This improved high-rate performance can be attributed to the introduction of the carbon interlayer. It can be acted as a conductive network, where the electrolyte was contained. The introduction of the carbon interlayer will facilitate the transfer of lithium ion and electron, and largely reduce the charge transfer resistance.

The charge-discharge curves of the cell with or without the carbon interlayer between 2.5 V and 4.2 V voltage limits at different current density are shown in Fig. 4c and 4d. It can be seen that the specific capacity and discharge voltage declined with an increase of the current density. As shown in Fig. 4c, the cell with the carbon interlayer can maintain the higher and longer discharge plateau than that of the cell without the carbon interlayer, especially at higher discharge current density. The smaller potential separation between the charge and discharge plateaus indicates better kinetics characteristics and better reversibility of the cell with the carbon interlayer, which can be ascribed to the lower potential polarization of the $LiFePO_4$ cell during the charge and discharge processes [31].

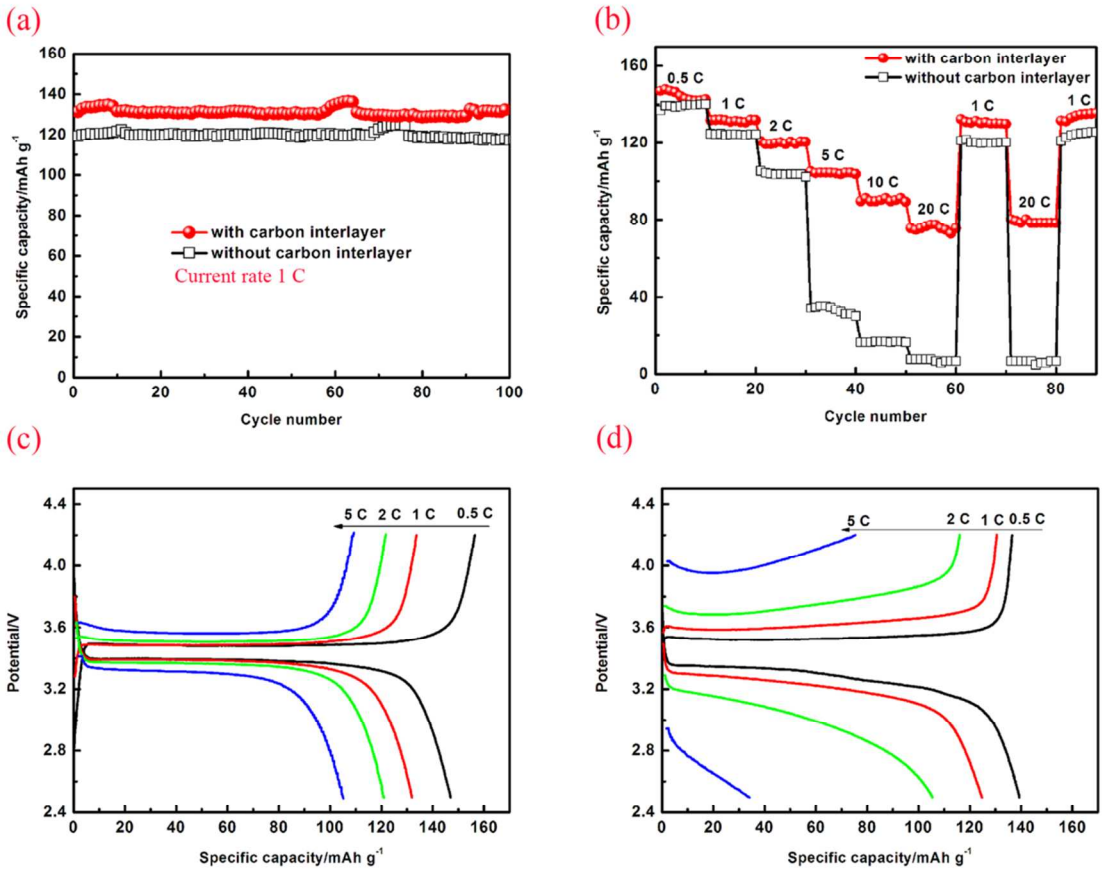

Fig. 4 Cycle performance of the $LiFePO_4$ cell with and without the carbon interlayer at 1 C (1 C = 170 mA g^{-1}) (a); Rate performance of the $LiFePO_4$ cell with and without the carbon interlayer (b); Charge-discharge profiles of the $LiFePO_4$ cell with (c) and without the carbon interlayer (d) at different current density

To further investigate the effect of carbon interlayer on the cycle performance of the $LiFePO_4$ cell at high current density, cycle performance test was carried at 2 C and 5 C. As shown in Fig. 5, the cell with the carbon interlayer shows better cycle stability than the cell without the carbon interlayer. The discharge capacity of the cell without the carbon interlayer is 112 mAh g^{-1} for the initial cycle and decreases to 79 mAh g^{-1} after 100 cycles at 2 C, which is similar to the other result [32]. Whereas the discharge capacity of the cell with the carbon interlayer is 128 mAh g^{-1} for the initial cycle and a high reversible capacity of 124.5 mAh g^{-1} is retained after 100 cycles with the capacity retention ratio of 97.3%, showing a great improvement in cyclability. With the introduction of the carbon interlayer, the electrochemical performance is significantly improved at high current density (5 C). The initial specific capacity is 107 mAh g^{-1}, even after 500 cycles, over 70% capacity retention is achieved, and a decay rate of 0.06% per cycle is estimated. However, the cell without the carbon interlayer rarely delivers any capacity after a long cycles.

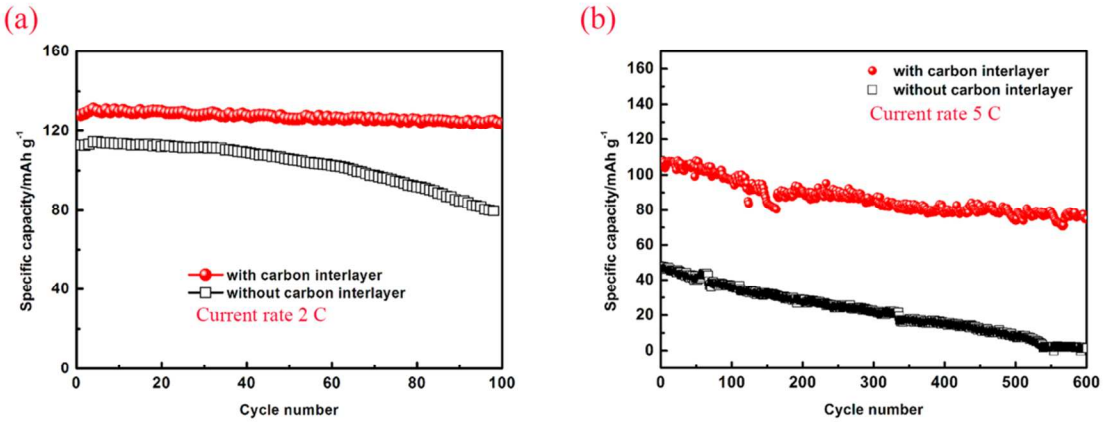

Fig. 5 Cycle performance of $LiFePO_4$ cell with and without the carbon interlayer at 2 C (a) and 5 C (b)

In order to explain the improved electrochemical performance of the $LiFePO_4$ cell with the carbon interlayer, electrochemical impedance spectroscopy (EIS) measurements were carried out before cycling (Fig. 6). The impedance plots are composed of a depressed semicircle at high frequency, which corresponds to the charge transfer resistance (Rct) of the $LiFePO_4$ cell [33], and an inclined line at low frequency, which reflects the Li ion diffusion into the active mass [34]. It is clear that the charge transfer resistance (Rct) of the cell with the carbon interlayer is much smaller than that of the cell without the carbon interlayer. The low resistance arises from the conductive carbon interlayer, resulting in a better rate capability and a higher reversible capacity, similar to the phenomenon are found in other works using interlayer.

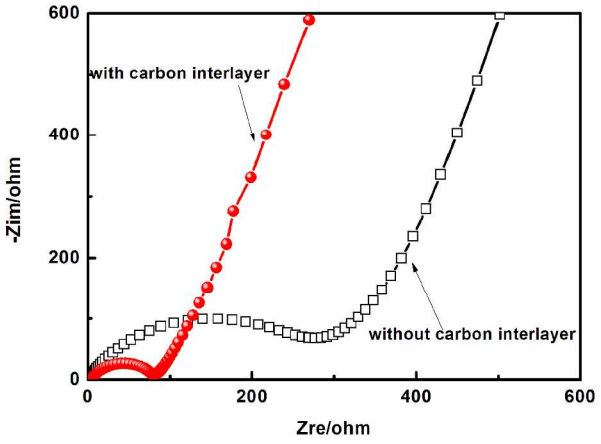

Fig. 6 Nyquist plots for the fresh $LiFePO_4$ cell with and without the carbon interlayer

Conclusions

In conclusion, the novel configuration of inserting a carbon interlayer into the $LiFePO_4$ battery significantly enhances both the rate performance and the cycle stability. The carbon interlayer as a conductive network largely can reduce the charge transfer resistance. Consequently, The $LiFePO_4$ battery with the carbon interlayer can deliver a high specific capacity of 90 mAh g^{-1} and 76 mAh g^{-1} at 10 C and 20 C, respectively. The design of inserting a conductive carbon interlayer into $LiFePO_4$ battery is a simple and effective new approach, and we believe this strategy can be extended to other lithium ion battery.

Notes and references

[a] *School of Metallurgy and Environment, Central South University, Changsha 410083, China. Fax: +86 731 88830649; Tel: +86 731 88830649; E-mail: zza75@163.com(Z Zhang) laiyanqingcsu@163.com(Y Lai)*

1. T. M. Bandhauer, S. Garimella, and T. F. Fuller, *J. Electrochem. Soc.*, 2011, 158, R1-R25
2. B. Kang, and G. Ceder, *Nature*, 2009, 458, 190-193.
3. P. G. Bruce, B. Scrosati, and J. M. Tarascon, *Angew. Chem. Int. Ed.*, 2008, 47, 2930-2946.
4. S. Q. Chen, P. Chen, M. H. Wu, D. Y. Pan, and Y. Wang, *Electrochem. Commun.*, 2010, 12, 1302-1306.
5. M. R. Hill, G. J. Wilson, L. Bourgeois, and A. G. Pandolfo, *Energy Environ. Sci.*, 2011, 4, 965-972.
6. A. Vu, and A. Stein, Chem. Mater., 2014, 23, 3237-3240.
7. S. L. Yang, X. F. Zhou, J. G. Zhang, and Z. P. Liu, *J. Mater. Chem.*, 2010, 20, 8086-8091.
8. D. Jugovic, and D. Uskokovic, *J. Power Sources*, 2009, 190, 538-544.
9. M. S. Islam, D. J. Driscoll, C. A. Fisher, and P. R. Slater, *Chem. Mater.*, 2005, 17, 5058-5062.
10. L. Wang, G. C. Liang, X. Q. Ou, X. K. Zhi, and J. P. Zhang, *J. Power Sources*, 2009, 189, 423-428.
11. J. J. Wang, X. L. Sun, *Energy Environ. Sci.*, 2012, 5, 5163-5185.
12. J. J. Wang, X. L. Sun, *Energy Environ. Sci.*, 2015, DOI: 10.1039/C4EE04016C.
13. L. Shen, H. Li, E. Uchaker, X. Zhang, and G. Cao, *Nano Lett.*, 2012, 12, 5673-5678.
14. Y. Kadoma, J. M. Kim, K. Abiko, K. Ohtsuki, and K. Ui, *Electrochim. Acta*, 2010, 55, 1034-1041.
15. J. J. Wang, J. L. Yang, Y. Zhang, Y. L. Li, Y. J. Tang, M. N. Banis, X. F. Li, G. X. Liang, R. Y. Li, X. L. Sun, *Adv. Funct. Mater.*, 2013, 23, 806-814.
16. H. Li, and H. Zhou, *Chem. Commun.*, 2012, 48, 1201-1217.
17. J. Chen, D. L. M. Yan, and B. H. Yue, *J. Power Sources*, 2012, 209, 7-14.
18. J. L. Yang, J. J. Wang, Y. J Tang, D. X. Wang, X. F. Li, Y. H. Hu, R. Y. Li, G. X. Liang, T. K. Sham, X. L. Sun, *Energy Environ. Sci.*, 2013, 6, 1521-1528.
19. A. Yamada, S. C. Chung, and K. Hinokuma, *J. Electrochem. Soc.*, 2001, 148, A224-A229.
20. S. B. Lee, S. H. Cho, S. J. Cho, G. J. Park, and Y. S. Lee, *Electrochem. Commun.*, 2008, 10, 1219-1221.

21. M. Konarova, and I. Taniguchi, *J. Power Sources*, 2010, 195, 3661-3667.
22. J. J. Wang, J. L. Yang, Y. J. Tang, J. Liu, Y. Zhang, G. X. Liang, M. Gauthier, Y. K. Wiegart, M. N. Banis, X. F. Li, R. Y. Li, J. Wang, T. K. Sham, X. L. Sun, *Nat. Commun.*, 2014, 5, 3415.
23. H. Zheng, R. Yang, G. Liu, X. Song, and V. S. Battaglia, *J. Phys. Chem. C*, 2012, 116, 4875-4882.
24. Z. Zhang, T. Zeng, Y. Lai, M. Jia, and J. Li, *J. Power Sources*, 2014, 247, 1-8.
25. Y. H. Qu, Z. Zhang, Z. W. Wang, Y. Lai, Y. X. Liu, and J. Li, *J. Mater. Chem. A,* 2013, *1*, 14306-14310.
26. J. Robertson, Mater. Sci. Eng. R, 2002, 37, 129-281.
27. L. X. Liao, X. Q. Cheng, Y. L. Ma, P. J. Zuo, W. Feng, G. P. Yin, and Y. Z. Gao, *Electrochim. Acta*, 2013, 87, 466-472.
28. N. A. Hamid, S. Wennig, S. Hardt, A. Heinzel, C. Schulz, and H. Wiggers, *J. Power Sources*, 2012, 216, 76-83.
29. L. Wang, X. M. He, W. T. Sun, J. L. Wang, Y. D. Li, and S. S. Fan, *Nano Lett.*, 2012, 12, 5632-5636.
30. J. Ha, S. K. Park, S. H. Yu, A. Jin, B. Jang, S. Bong, I. Kim, Y. Sung, and Y. Piao, *Nanoscale*, 2013, 5, 8647-8655.
31. H. Shu, X. Wang, Q. Wu, B. Ju, L. Liu, X. Yang, Y. Wang, Y. Bai, and S. Yang, *J. Electrochem. Soc.*, 2011, 158, A1448-A1454.
32. C. H. Yim, Elena Baranova, Y. Lebdeh, and I. Davidson, *J. Power Sources*, 2012, 205, 414-419.
33. Y. Wang, R. Mei, and X. Yang, *Ceram. Int.*, 2014, 40, 8439-8444.
34. F. Gao, and Z. Tang, *Electrochim. Acta*, 2008, 53, 5071-5075.